Epitaxial Growth and Characterization of (001) Cd_3As_2 Thin Films on a Lattice Matched Buffer

By Julie Lampert

Lynbrook Senior High School

Abstract

Cadmium arsenide (Cd_3As_2) is a three-dimensional (3D) Dirac semimetal that has been shown to exhibit electrical transport properties such as high carrier mobility, ultrahigh magnetoresistance, and topological surface states. This makes Cd_3As_2 a promising candidate for use in future electronic technologies such as quantum computers, spintronics devices, photo and infrared detectors, and more. While previous experiments have studied epitaxially grown Cd_3As_2 heterostructures, the characteristics of (001) oriented films grown on lattice matched buffer layers have yet to be explored. This project investigates the growth and electronic properties of Cd_3As_2 films grown on an $Al_{(.42)}In_{(.58)}Sb$ buffer layer, deposited on a GaSb substrate. This study reveals that this novel heterostructure can be grown successfully and has a similar carrier mobility and slightly lower carrier density than films with lattice mismatched buffer layers. Shubnikov-de Haas oscillations and the onset of the quantum Hall effect are also observed. These findings allow for a better understanding of Dirac semimetals and pave the way for new materials with impactful electronic applications.

Introduction

Cadmium arsenide (Cd_3As_2) is a well-known semiconducting material that has recently been classified as a three-dimensional (3D) Dirac semimetal, a newly discovered category of quantum matter [1]. The electronic band structure of Dirac semimetals is an intermediate state between insulators and metals, in which the valence and conduction bands cross at discrete points in momentum space called Dirac nodes [2]. A visual representation of this band structure can be seen in Fig.1. While these point-like degeneracies have previously been observed in spineless graphene, a two-dimensional (2D) system, it was only recently that a 3D analog was experimentally realized [3,4]. The four-fold rotational symmetry of the tetragonal crystal structure of Cd_3As_2 protects the Dirac nodes, even at high Fermi energies [2,4]. The non-trivial topology of Cd_3As_2 along with its unique band structure generates surface states similar to that of 3D topological insulators, as required by the Z_2 invariant. This means that when a bandgap opens in the bulk of the material, metallic surface states will arise [6].

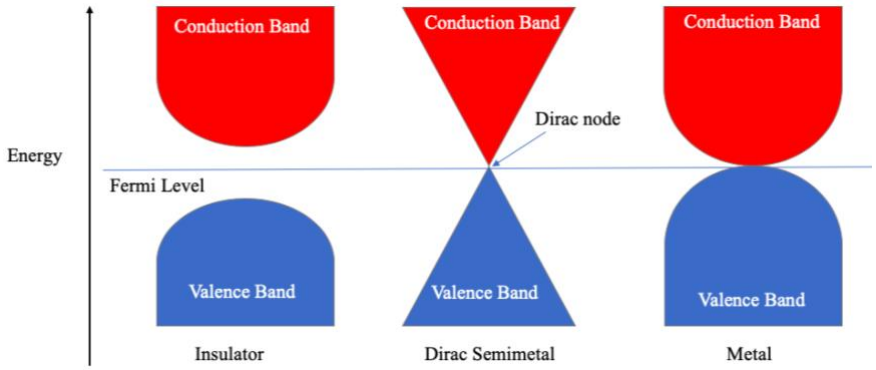

FIG.1. Schematic comparing the band structure of Dirac semimetals to that of insulators and metals

While a variety of other Dirac semimetals have been discovered, Cd_3As_2 is the only one known to be electrochemically stable at room temperature. Because of this, Cd_3As_2 is compatible with the conditions in functional electronic devices. Additionally, the Fermi level of Cd_3As_2 can be adjusted, allowing it to be utilized across a wide range of technological applications [7]. A recent study found that Cd_3As_2 could be tuned to a topological superconducting state when placed under high pressure conditions [8]. Topological superconductors are a known source of Majorana fermions: quasiparticles which can be used in quantum computers. The linear band dispersion and zero bandgap of Cd_3As_2, along with its high carrier mobility, give it a high responsivity to electromagnetic waves. This is a necessary quality for materials used in infrared and photodetectors [9]. Spin polarization of carriers is also possible in Cd_3As_2, making it a possible candidate for use in spintronics devices [10].

The magnetotransport properties of Cd_3As_2 thin films are especially unusual. Electronic phenomena such as ultrahigh magnetoresistance and negative magnetoresistance have been observed [11]. The longitudinal (R_{xx}) resistance of Cd_3As_2 thin films placed under strong magnetic fields at low

temperatures shows Shubnikov-de Haas quantum oscillations. The Hall (R_{xy}) resistance of these films shows the quantum Hall effect, which confirms the carrier dominance of 2D edge states, and gives insight into the details of the electronic structure of the material [12]. Cd_3As_2 has also been found to have ultrahigh carrier mobility, an especially sought-after property in electronic materials. Mobility values of up to 10^7 cm^2 /Vs have been observed for Cd_3As_2 single crystals at low temperatures under weak magnetic fields, and mobilities of 9×10^6 cm^2 /Vs have been observed in zero magnetic fields. For reference, this is comparable to the highest recorded mobility in a 2D electron gas (3.6×10^7 cm^2 /Vs) [13].

Manipulation of different aspects of Cd_3As_2 heterostructures allows for the properties of the films to be tuned. The buffer on which the Cd_3As_2 films are deposited is known to have effects on the film's properties. One study subjected Cd_3As_2 films to both compressive and tensile strain by varying the lattice parameter of a $Ga_{(1-x)}In_{(x)}Sb$ buffer layer [14]. Another study found that the surface morphology of the films could be improved through the use of an InAs wetting layer [15]. While buffer layers have been used to improve Cd_3As_2 films, they can also have negative impacts on the film's quality. A buffer layer with a mismatched lattice parameter may cause dislocations, which can lower the electron mobilities in thin films [16]. The orientation of the film growth can also be changed. The presence of Fermi arcs on the surface of Cd_3As_2 films grown in the (112)-orientation has been observed in momentum space. The arcs create a tunnel-like path through the Dirac nodes, allowing conduction through a Fermi loop [5]. While (001)-oriented films have been grown successfully, better established (112) orientations are more widely studied [15]. The (001) orientation differs from that of the (112) direction in that the two Dirac nodes project onto a single point [7].

Great progress has been made in the understanding and improvement of the electronic properties of Cd_3As_2 in recent years. Despite this development, much is still unknown about this material. In this investigation, we seek to explore the electrical transport qualities of (001) Cd_3As_2 films grown epitaxially on an $Al_{(.42)}In_{(.58)}Sb$ lattice matched buffer layer deposited on a GaSb substrate. This will create a novel heterostructure with minimal dislocations in the Cd_3As_2 layer. In addition, $Al_{(.42)}In_{(.58)}Sb$ and GaSb have bandgaps higher than Cd_3As_2. This will allow for the electrical transport of Cd_3As_2 to be studied without interference from these layers. The goal of this study is to create a film with enhanced electrical transport as compared to films on lattice mismatched buffers, which often have dislocations, and to gain insight into the effect of buffer composition and orientation on carrier mobility and carrier density of thin Cd_3As_2 films.

Methods

Thin films were grown using molecular beam epitaxy (MBE) under ultrahigh vacuum conditions (10^{-10} mTorr). MBE was selected as the growth method because it is a low energy process, allowing for a greater degree of control over film growth a apposed to other methods like laser deposition [17]. A (001) GaSb wafer was first heated to 510 °C to desorb oxides under Sb flux. Then, a 50 nm thick (001) GaSb layer was deposited on the substrate to provide a clean interface for the next layer. A 700 nm thick layer of (001) $Al_{(.42)}In_{(.58)}Sb$ was then grown on the GaSb. Finally, (001) Cd_3As_2 was grown for 100 sec (40 nm). Reflection high-energy electron diffraction (RHEED) was used to monitor film growth *in situ*. The finer details of this procedure have been reported elsewhere [17]. The Panalytical MRD PRO Diffractometer was used to carry out x-ray diffraction (XRD) and x-ray reflectivity (XRR), with Cu Kα (1.5405 Å) radiation. Out-of-plane 2θ-ω XRD scans were taken in the (004) plane to avoid overlap of the Cd_3As_2 and $Al_{(.42)}In_{(.58)}Sb$ peaks. Bragg's law was used to determine the lattice parameter of each layer, and Vegard's law was used to calculate the buffer composition. X-ray reflectivity (XRR) measurements were used to calculate the thickness of the Cd_3As_2 layer. Atomic force microscopy images allowed for analysis of the surface morphology of both the buffer layer and Cd_3As_2 layer. After film characterization, Hall bar devices were constructed in the cleanroom and processed via Ar ion milling. Carrier density and carrier mobility measurements were taken in a Quantum Design Physical Properties Measurements Dynacool system under magnetic fields (-0.5 T to 0.5 T) at low temperatures (2 K to 20 K). Magnetoresistance measurements were taken at 2K under magnetic fields of -9 T to 9 T.

Results & Discussion

The streaky pattern on the RHEED images indicates that both film layers had the desired 2D nucleation during growth (Fig.2). The lattice parameter of the buffer layer calculated based on the Bragg angle is a = 6.34 Å. The composition of the buffer was calculated to be 58% aluminum and 42% indium Vegard's law. The values used in the calculation for the lattice parameters of aluminum antimonide (AlSb) and indium antimonide (InSb) were a = 6.10 Å and a = 6.48 Å, respectively [18,19]. The XRD scan in Fig.3 shows the angle of highest intensity for each layer of the film. The GaSb substrate has a much higher intensity than the other two layers due to its ~3 mm thickness. The lattice parameter of Cd_3As_2 is 6.38 Å, a 0.5% lattice mismatch from the buffer (6.34 Å). The overlap of the Cd_3As_2 and buffer peaks indicates a lattice match. AFM images of the $Al_{(.42)}In_{(.58)}Sb$ buffer and the Cd_3As_2 layer can be seen in Fig.4. The root-mean-square roughness values are 2.37 nm for the buffer layer and 2.23 nm for Cd_3As_2. These values confirm the desired smooth surface morphology. The similarity of the root-mean-square roughness values of the buffer and Cd_3As_2 layer indicates that the surface morphology of the buffer directly affects that of the Cd_3As_2. The thickness of the Cd_3As_2 layer is calculated to be 40 nm using XRR (Fig.5). Transport measurements from a (001)-oriented 45 nm thick Cd_3As_2 film grown on a $Ga_{(.20)}Al_{(.80)}Sb_{(.91)}As_{(.09)}$ buffer have been reported previously [15]. A comparison of this film to the lattice matched film can be seen in

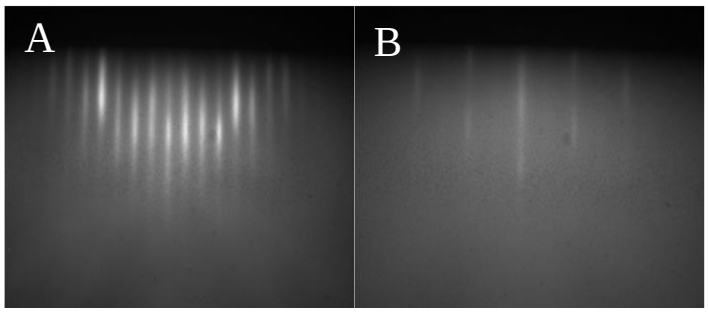

FIG.2. (A) RHEED image of the $Al_{(.42)}In_{(.58)}Sb$ buffer layer. (B) RHEED image of the Cd_3As_2 film. Streaks seen in both images indicate 2D nucleation.

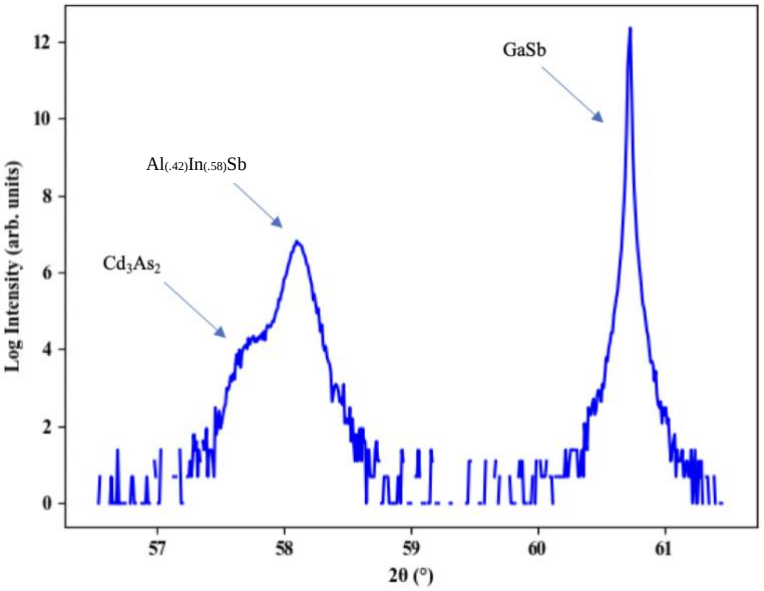

FIG.3. Out-of-plane (004) 2θ-ω XRD scan of the lattice matched Cd_3As_2 heterostructure. The lattice parameters of each layer were determined to be a= 6.092 Å for GaSb, a = 6.343 Å for $Al_{(.42)}In_{(.58)}Sb$, and a = 6.379 Å for Cd_3As_2. The lattice mismatch between the Cd_3As_2 and the buffer layer is 0.5%

Table 1. The lattice matched film showed a lower carrier density than the mismatched film, which may be indicative of a higher degree of quality. This is because dislocations cause the Fermi level to deviate from the Dirac nodes, moving to a higher density of states. This allows for more carriers to occupy these states, resulting in an increase in carrier density. While it is expected that higher quality films will have increased carrier mobility, the observed carrier mobility of the lattice matched film is in the same range as the mismatched films. Nonetheless, this value still shows that lattice matched films have mobilities comparable to mismatched films. It is important to note that the bandgap of both the buffer layer and substrate is greater than that of Cd_3As_2. This reduces the possibility of contribution to carrier density by these layers [20]. The transport data for both carrier mobility and carrier density is shown only for low temperatures because thermal excitations in the buffer and substrate layers cause interference above 20 K. Fig.6 shows the magnetoresistance measurements of the film. The observation of the quantum Hall effect confirms 2D transport at low

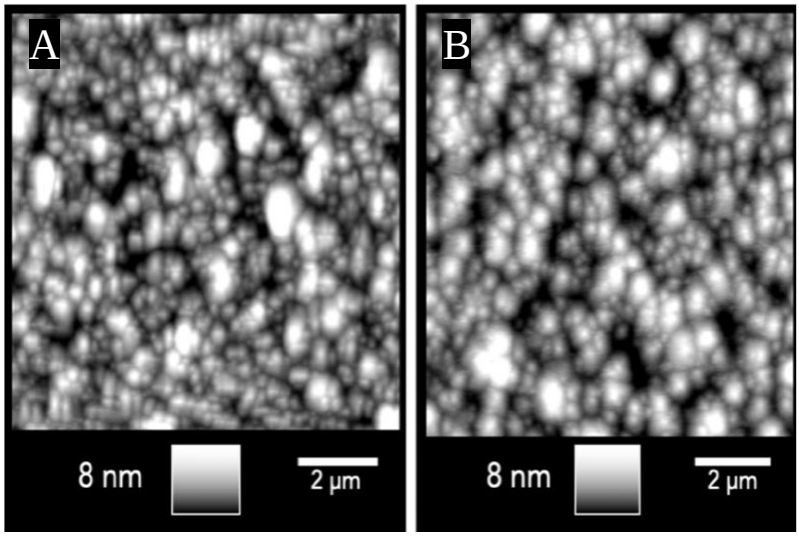

FIG.4.(A) AFM image of the Cd_3As_2 film. The root-mean- square roughness value is 2.23 nm. (B) AFM image of the $Al_{(.42)}In_{(.58)}Sb$ buffer layer taken before Cd_3As_2 growth. The root-mean-square roughness value is 2.37 nm

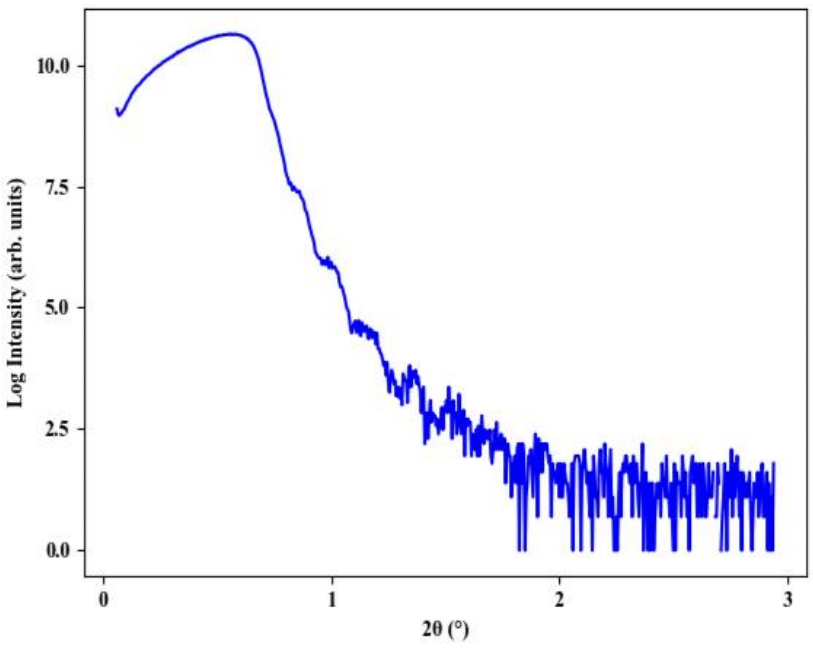

FIG.5. Out-of-plane XRR scan of the Cd_3As_2 film. The thickness of the Cd_3As_2 layer (grown for 100 sec) was determined to be 40 nm.

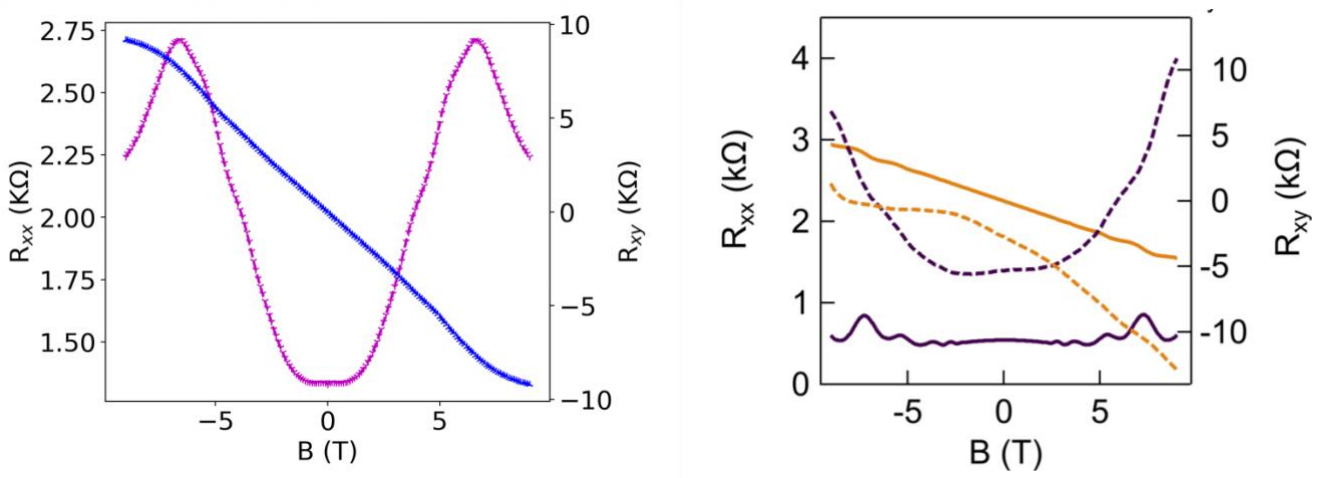

FIG.6. (A) Magnetoresistance of the film. The purple line shows the longitudinal resistance (R_{xx}) and the blue shows the Hall resistance (R_{xy}). Shubnikov-de Haas oscillations can be seen in the longitudinal resistance and the onset of quantum Hall plateaus can be seen in the Hall resistance. (B) Magnetoresistance of the lattice mismatched buffer film (Kealhofer et al.). The dashed purple line shows the R_{xx} and the dashed yellow line shows the R_{xy}. The solid lines show results for a film treated with N* plasma and should be disregarded.

temperatures, and Shubnikov-de Haas oscillations indicate that the film is high quality. The longitudinal resistance is more symmetrical than that of the lattice mismatched film, and the Hall resistance is more asymmetrical. This further confirms that the lattice matched film has higher crystal quality.

Lattice Mismatch	Carrier Density	Carrier Mobility
-4%	1.0×10^{12} cm^{-2}	9,300 cm^2 /Vs
.05%	5.8×10^{11} cm^{-2}	8,050 cm^2 /Vs

TBL.1. Comparison of transport data from a previously reported film on a lattice mismatched buffer (Schumann et. al.) and the lattice matched film.

Conclusion and Future Work

In this study we show that lattice matched (001) Cd_3As_2 films can successfully be grown epitaxially on an $Al_{(.42)}In_{(.58)}Sb$ buffer layer. The surface morphology of the Cd_3As_2 film is influenced significantly by the roughness of the buffer layer. A slight decrease in the carrier density indicates that lattice matched films can reach a higher level of quality than films grown on lattice mismatched buffers. The improvement of the purity of Cd_3As_2 films shown in this experiment is an important step in creating materials with the capabilities to be used in future technologies. By treating the top surface of these Hall bar devices with N* plasma, the non-dominant carrier type (*p*-type) can be eliminated, resulting in high mobility, single-carrier transport [20]. The observation of a direct correlation between the root-mean-square roughness value of the buffer and Cd_3As_2 layer indicates that the surface morphology of the Cd_3As_2 layer can be improved by manipulating the buffer. Additionally, the mismatch between the buffer and Cd_3As_2 layer is 0.5%. While this value is significantly lower than the lattice mismatched film, it leaves room for improvement. An avenue of future studies is the growth of heterostructures with multiple buffer layers to more accurately match the lattice parameter of Cd_3As_2. These higher purity films may possess improved transport properties, as indicated by the increase in carrier mobility from lattice match to lattice mismatch films. Furthermore, higher quality films can also be realized by utilizing different methods of epitaxial growth such as step-flow or layer-by-layer growth.

References

[**1**] Young, S., Zaheer, S., Teo, J., Kane, C., Mele, E. and Rappe, A. (2012). Dirac Semimetal in Three Dimensions. *Physical Review Letters*, 108(14).

[**2**] Liu, Z., Jiang, J., Zhou, B., Wang, Z., Zhang, Y., Weng, H., Prabhakaran, D., Mo, S., Peng, H., Dudin, P., Kim, T., Hoesch, M., Fang, Z., Dai, X., Shen, Z., Feng, D., Hussain, Z. and Chen, Y. (2014). A stable three- dimensional topological Dirac semimetal Cd3As2. *Nature Materials*, 13(7), pp.677-681.

[**3**] Young, S. and Kane, C. (2015). Dirac Semimetals in Two Dimensions. *Physical Review Letters*, 115(12).

[**4**] Borisenko, S., Gibson, Q., Evtushinsky, D., Zabolotnyy, V., Büchner, B. and Cava, R. (2014). Experimental Realization of a Three-Dimensional Dirac Semimetal. *Physical Review Letters*, 113(2).

[**5**] Wang, C., Sun, H., Lu, H. and Xie, X. (2017). 3D Quantum Hall Effect of Fermi Arcs in Topological Semimetals. *Physical Review Letters*, 119(13).

[**6**] Yang, B. and Nagaosa, N. (2014). Classification of stable three-dimensional Dirac semimetals with nontrivial topology. *Nature Communications*, 5(1).

[**7**] Wang, Z., Weng, H., Wu, Q., Dai, X. and Fang, Z. (2013). Three-dimensional Dirac semimetal and quantum transport in Cd3As2. *Physical Review B*, 88(12).

[**8**] He, L., Jia, Y., Zhang, S., Hong, X., Jin, C. and Li, S. (2016). Pressure-induced superconductivity in the three-dimensional topological Dirac semimetal Cd3As2. *npj Quantum Materials*, 1(1).

[**9**] Wang, Q., Li, C., Ge, S., Li, J., Lu, W., Lai, J., Liu, X., Ma, J., Yu, D., Liao, Z. and Sun, D. (2017). Ultrafast Broadband Photodetectors Based on Three- Dimensional Dirac Semimetal Cd3As2. *Nano Letters*, 17(2), pp.834-841.

[**10**] Yang, S. (2016). Dirac and Weyl Materials: Fundamental Aspects and Some Spintronics Applications. *SPIN*, 06(02), p.1640003.

[**11**] Schumann, T., Goyal, M., Kealhofer, D. and Stemmer, S. (2017). Negative magnetoresistance due to conductivity fluctuations in films of the topological semimetal Cd3As2. *Physical Review B*, 95(24).

[**12**] Schumann, T., Galletti, L., Kealhofer, D., Kim, H., Goyal, M. and Stemmer, S. (2018). Observation of the Quantum Hall Effect in Confined s of the Three- Dimensional Dirac Semimetal Cd3As2. *Physical Review Letters*, 120(1).

[13] Liang, T., Gibson, Q., Ali, M., Liu, M., Cava, R. and Ong, N. (2014). Ultrahigh mobility and giant magnetoresistance in the Dirac semimetal Cd3As2. *Nature Materials*, 14(3), pp. 280-284.

[**14**]Goyal, M., Kim, H., Schumann, T., Galletti, L., Burkov, A. and Stemmer, S. (2019). Surface states of strained thin films of the Dirac semimetal Cd3As2. *Physical Review Materials*, 3(6).

[**15**] Kealhofer, D., Kim, H., Schumann, T., Goyal, M., Galletti, L. and Stemmer, S. (2019). Basal-plane growth of cadmium arsenide by molecular beam epitaxy. *Physical Review Materials*, 3(3).

[16] Lebedev, V., Cimalla, V., Baumann, T. and Ambacher, O. (2019). Effect of dislocations on electrical and electron transport properties of InN thin films. II. Density and mobility of the carriers: *Journal of Applied Physics*: Vol 100, No 9.

[17] Schumann, T., Goyal, M., Kim, H. and Stemmer, S. (2016). Molecular beam epitaxy of Cd3As2 on a III-V substrate. *APL Materials*, 4(12), p.126110.

[18] Straumanis, M. and Kim, C. (2019). Lattice Parameters, Thermal Expansion Coefficients, Phase Width, and Perfection of the Structure of GaSb and InSb.

[19] Jamieson, J. (1963). Crystal Structures at High Pressures of Metallic Modifications of Compounds of Indium, Gallium, and Aluminum. *Science*, 139(3557), pp.845-847

[20] Galletti, L., Schumann, T., Mates, T. and Stemmer, S. (2018). Nitrogen surface passivation of the Dirac semimetal Cd3As2. *Physical Review Materials*,